

# Optimization design and experiment on ripple surface type pickup finger of precision maize seed metering device

Wang Jinwu\*, Tang Han, Wang Jinfeng, Li Xin, Huang Huinan

(College of Engineering, Northeast Agricultural University, Harbin 150030, China)

**Abstract:** A ripple surface type pickup finger was designed to improve the performance of pickup finger precision maize seed metering device and to provide a solution for precision maize planter. The main structure and working principle of seed metering device were detailed in this paper. The dimension size distributions of maize seeds in different types were studied, the gestures of seeds clamped by pickup finger were analyzed, and the clamping dynamical model of pickup finger was established by theoretical analysis. To optimize the structural parameters of ripple surface type pickup finger, the discrete element method (DEM) model of pickup finger precision maize seed metering device was established by the discrete element software EDEM. The numerical simulations of orthogonal seeding performance experiments were conducted to analyze the influences of these factors on the quality of seeding. The rotational speed, wavelength of ripple surface and amplitude of ripple surface were selected as the experimental factors. The average seeding qualified index and the average seeding coefficient of variation on four different types of maize seeds were chosen for evaluating the seeding performance. The results showed that, the average seeding qualified index was 93.35% and the average seeding coefficient of variation was 11.23% under conditions of the 25 r/min rotational speed, 8 mm wavelength of ripple surface and 2 mm amplitude of ripple surface. Under the same condition, the bench test was done which showed that the results of test and simulation were consistent. The maximum error of qualified index was 1.95% and the qualified index of improved seed metering device exceeded the original one by 12.34%. The working performance can meet the requirements of precision maize seeding.

**Keywords:** precision maize planter, seed metering device, pickup finger, ripple surface

**DOI:** 10.3965/j.ijabe.20171001.2050

**Citation:** Wang J W, Tang H, Wang J F, Li X, Huang H N. Optimization design and experiment on ripple surface type pickup finger of precision maize seed metering device. *Int J Agric & Biol Eng*, 2017; 10(1): 61–71.

## 1 Introduction

The pickup finger precision maize seed metering

**Received date:** 2016-09-15 **Accepted date:** 2016-12-05

**Biographies:** **Tang Han**, PhD candidate, research interests: agricultural mechanization engineering and precision planting technology, Email: tanghan19910102@163.com; **Wang Jinfeng**, PhD, Associate Professor, research interests: agricultural mechanization engineering, Email: jinfeng\_w@126.com; **Li Xin**, Master student, research interests: agricultural mechanization engineering, Email: 1103829924@qq.com; **Huang Huinan**, Master student, research interests: agricultural mechanization engineering, Email: 1258081488@qq.com.

**\*Corresponding author:** **Wang Jinwu**, PhD, Professor, research interests: farm machine and mechanical reliability. Mailing address: Engineering College, Northeast Agricultural University, Harbin, Heilongjiang 150030, China. Tel: +86-451-55191188, Email: jinwu@163.com.

device is a kind of major mechanical seed metering device, which has already been increasingly widespread<sup>[1]</sup> in China for the advantages of high planting quality, simple structure and low seed-injuring rate. Pickup finger is the core part of seed metering device, which directly contacts with maize seeds, clamps and pushes for achieving the process of seed-filling. The structural shapes and dimension parameters of pickup finger have great influences on seeding quality. In operation, pickup fingers ride on a stationary cam with fine springs, as they travel to the bottom of filling shell, pickup fingers will open in sequences, and each finger picks up one or more maize seeds. With further movement, pickup finger passes across guiding hole and the seed is ejected into guiding belt for transport to seed tube. Many scholars<sup>[2,3]</sup> around the world have conducted researches on the

development of pickup finger seed metering device. Wang et al.<sup>[4,5]</sup> designed a new kind of pickup finger precision maize seed metering device based on theoretical analysis and virtual simulation. And a mathematical model based on the test of quadratic general rotary unitized design was built to optimize its working performance. Meanwhile, the seed metering device was great affected by the shape and size of maize seeds in actual field. This shortage has greatly restricted its expanded application.

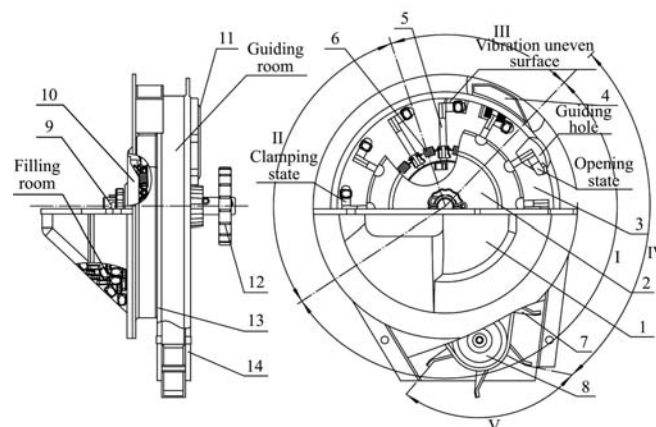
At present, maize seeds are divided into 6 grades by manual classification of cleaning according to the shape and size in foreign planting industries, and maize seeds are generally divided into 2-3 grades in China<sup>[6-8]</sup>. Due to varieties of the shape and size of maize seeds, and under condition of morphological transform process, the clamping performance of pickup finger degrades which results in the slipping of seeds and the low efficiency of operations. Thus, the original pickup finger precision maize seed metering device cannot entirely meet the technical requirements of precision seeding.

In this case, in order to solve the mentioned problems above and to improve the seeding performance, we dealt with the dimension size distributions of maize seeds in different types, analyzed gestures of seeds clamped by pickup finger, and established clamping dynamical model of pickup finger. Then a ripple surface type pickup finger was designed. On this basis, the discrete element method (DEM) model<sup>[9,10]</sup> of pickup finger precision maize seed metering device was established by the discrete element software EDEM. The numerical simulations of orthogonal experiments on seeding performance were conducted. Then the bench test was also carried out to verify the truth and reliability of numerical simulations. This study can provide guidance and direction for design of mechanical precision seed metering device and its key component.

## 2 Structure and principle of metering device

As shown in Figure 1, the pickup finger precision maize seed metering device mainly consists of seed filling shell, pickup finger pin-plate, seed plate, clearing brush, pickup finger, fine spring, guiding belt, guiding

belt wheel, seeding shaft, setting cam, rubber mat for observation, driving sprocket, guiding end-cover, shield shell, etc. The seed metering device performs a whole working cycle through five sections, namely filling section, clamping section, clearing section, guiding section and dropping section. The specific working principle is shown in reference [4].



1. Seed filling shell 2. Pickup finger pin-plate 3. Seed plate 4. Clearing brush 5. Pickup finger 6. Fine spring 7. Guiding belt 8. Guiding belt wheel 9. Seeding shaft 10. Setting cam 11. Rubber mat for observation 12. Driving sprocket 13. Guiding end-cover 14. Shield shell I-Filling section II-Clamping section III-Clearing section IV-Guiding section V-Dropping section

Figure 1 Pickup finger precision maize seed metering device

## 3 Materials and methods

The dimension size and clamped gestures of maize seeds are important references in designing pickup finger. They also have main influences on the clamping performance and seeding adaptability. Therefore, this paper researched the dimension size distributions of maize seeds in different types, analyzed the gestures of seeds clamped by pickup finger using high speed photography technology.

### 3.1 Dimension size of maize seeds

In order to improve the seeding adaptability and reasonably design the structure parameters, the maize seeds of difference sizes and types were divided into four grades by manual classification of cleaning for test: big flat seed, small flat seed, big round seed and small round seed, as shown in Figure 2. One hundred seeds were picked out randomly from each type, and their length ( $L$ ), width ( $W$ ) and thickness ( $T$ ) were measured. The dimension size distributions are shown in Figure 3.

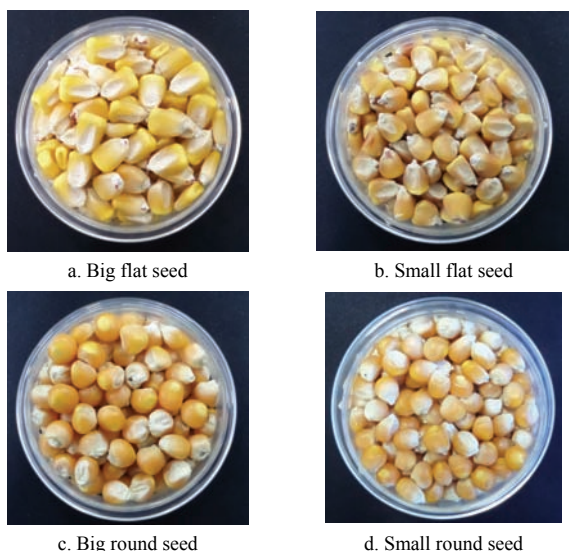


Figure 2 Four grades of maize seeds

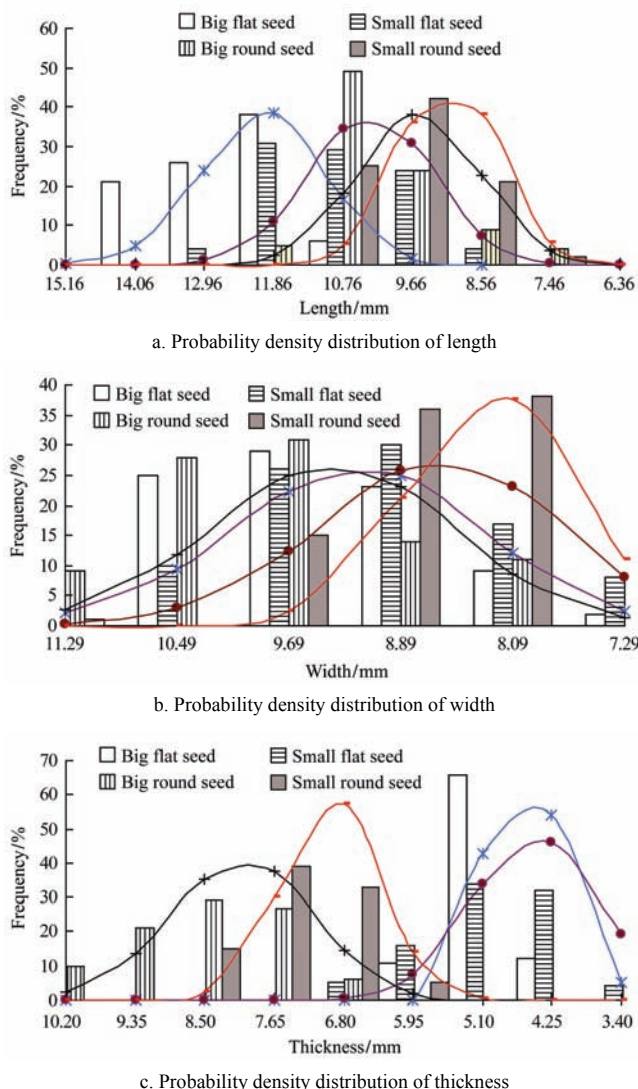


Figure 3 Probability density distributions of dimension size

The dimension size distributions of four different grades of maize seeds ranked in different ranges, while their dimension sizes all fit the moderate skew distributions (skewness coefficient  $\in [0.5,1]$ ). The

length ( $L$ ), width ( $W$ ) and thickness ( $T$ ) of big flat seed were mainly concentrated on 11-14 mm, 8-10 mm, 4-5.5 mm, their standard deviations were relatively larger, and the dimension distributions were disperse. The length ( $L$ ), width ( $W$ ) and thickness ( $T$ ) of small flat seed were mainly concentrated on 9-12 mm, 8-10 mm and 3-5 mm, their average size were relatively smaller than other two types. The length ( $L$ ), width ( $W$ ) and thickness ( $T$ ) of big round seed were mainly concentrated on 7-11 mm, 8-11 mm, 5-9 mm, their standard deviations were relatively smaller, and the dimension distributions were concentrated. The length ( $L$ ), width ( $W$ ) and thickness ( $T$ ) of small round seed were mainly concentrated on 8-10 mm, 7-9.5 mm and 6-8 mm.

### 3.2 Gestures of seeds clamped by pickup finger

The gestures of seeds clamped by pickup finger mainly include three forms, the direction of length, width and thickness respectively, they are proportional to the probability. By using high speed photography technology<sup>[11]</sup> under operating conditions (15-45 r/min), statistical analysis was conducted on the clamped gestures of 1000 maize seeds selected from four different grades randomly, as shown in Figure 4. The results showed that the probability of gestures for single seed clamped in the direction of length, width, thickness and the others were 37%, 27%, 22% and 14%, respectively.

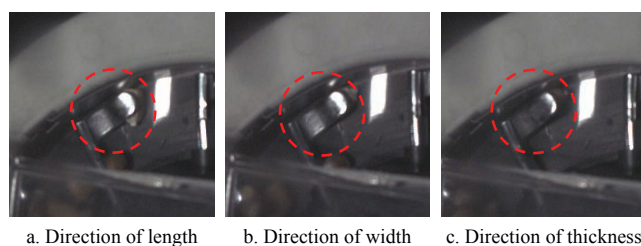
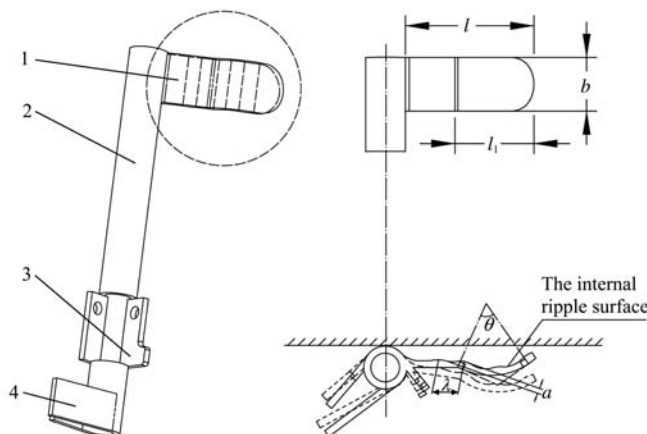


Figure 4 Diagram of the clamped gestures in different directions

Figure 4 shows that the clamping movements in the direction of width and thickness were relatively stable. These forms were the ideal clamped gestures which could ensure forces uniformly. The structure parameters of pickup finger should satisfy the clamping operation for different types of maize seeds, and the design of pickup finger arc-segment has important relation to the clamping force. Therefore, the three main clamped gestures were taken as boundary conditions for the design of structure parameters and position of pickup finger arc-segment.

### 3.3 Optimization design and analysis of pickup finger

Aimed for improving the clamping performance and stability of pickup finger, the clamping dynamical model was established according to the dimension size and clamped gestures of maize seeds. Then a ripple surface type pickup finger was optimally designed. The ripple surface type pickup finger consists of ripple finger clip, finger pole, finger lug and finger trail clip, as shown in Figure 5. Ripple finger clip is the core structure of pickup finger. Pickup finger and fine spring are connected and integrated by finger lug. Trail clip and setting cam control the opening space of pickup finger with contact fit, and support the whole pickup finger opening and closing. The key structural parameters of ripple surface type pickup finger include the length and width of clip  $l$  and  $b$ , the length and wrap angle of arc-segment  $l_1$  and  $\theta$ , the wave length and amplitude of ripple surface  $\lambda$  and  $a$ .



1. Ripple finger clip 2. Finger pole 3. Finger lug 4. Finger trail clip

Figure 5 Structural diagram of the pickup finger

The ripple finger clip was designed using with two arc-shaped segments to prevent the slipping and shedding of seeds in clamping process. Its external surface was designed to be space smooth surface to reduce collision and friction between seed groups and pickup finger in filling room, and its internal surface was designed to be small ripple surface. The design of whole structural parameters is related to the dimension size and clamped gestures of maize seeds. When the length of finger clip is too long, the clearing performance of seed metering device will be degraded, and then the multiple-seeding problem will arise. When the length of finger clip is too

short, the seeds slipping and shedding will be caused, and then the miss-seeding problem will arise. The width of finger clip should be greater than the average length of maize seeds to ensure the clamping stability in the direction of thickness. The length of finger arc-segment should be greater than the average length of maize seeds, and accounts for more than half of length of finger clip. The design principles are shown as follows:

$$\begin{cases} 2\bar{W}_0 > l > b > \bar{L}_0 \\ l_1 = (0.6 \sim 0.7)l \end{cases} \quad (1)$$

where,  $\bar{L}_0$  is the average length of maize seeds, mm;  $\bar{W}_0$  is the average width of maize seeds, mm.

The parameters of internal ripple surface are important factors to ensure the improvement of clamping performance. In the clamping and pushing processes, the internal ripple surface interacts with maize seeds in line contact. When mechanical vibration or collision among seeds generates, the direction of clamping force will change timely to reach forces system balance and ensure movement stability. The parameters of internal ripple surface are related to the overall sizes of pickup finger and maize seeds. The design principles are given by:

$$\begin{cases} 0.5l \geq \lambda \geq 0.6\bar{L}_0 \\ 0.4\bar{W}_0 \geq a \geq 0.5\bar{H}_0 \end{cases} \quad (2)$$

where,  $\bar{H}_0$  is the average thickness of maize seeds, mm.

According to the above equations and related data of the dimension size distributions, the structure parameters could be determined, the length of finger clip was  $l=20.0$  mm, the width of finger clip was  $b=11.5$  mm, the length of finger arc-segment was  $l_1=13.0$  mm, the wavelength of ripple surface was  $\lambda=(6.0-10.0)$  mm, the amplitude of ripple surface was  $a=(2.0-3.2)$  mm.

The wrap angle of finger arc-segment  $\theta$  is an important parameter for the stability of clamping. The clamping dynamical model of ripple surface type pickup finger was established to optimize the angle of arc-segment. The model was simplified from the actual clamping and pushing processes, as shown in Figure 6. Forces system on the clamped seed was analyzed in the limit position:

$$F_f = \mu_2 F_n \quad (3)$$

$$F_t = \mu_1 F_r \tag{4}$$

where,  $\mu_1$  is the friction coefficient between maize seeds and finger clip,  $\mu_1 \in (0.12, 0.35)$ ;  $\mu_2$  is the friction coefficient between maize seeds and seed plate,  $\mu_2 \in (0.30, 0.55)$ .

When the clamped seed is located in the limit position I, the forces in the vertical direction should reach balance, the dynamic analysis can be defined as following balance equation:

$$F_r \sin \alpha - F_t \cos \alpha = F_n \tag{5}$$

The relative static condition between single seed and finger clip should meet:

$$F_f \leq F_r \cos \alpha + F \sin \alpha \tag{6}$$

From Equations (3)-(6):

$$\alpha \geq \arctan \frac{1 + \mu_1 \mu_2}{\mu_2 - \mu_1} \tag{7}$$

When the clamped seed is located in the limit position II, the forces in the vertical direction should reach balance, the dynamic analysis can be defined as following balance equation:

$$F_r \sin \beta + F_t \cos \beta = F_n \tag{8}$$

The relative static condition between single seed and finger clip should meet:

$$F_f \leq F_r \cos \beta - F_t \sin \beta \tag{9}$$

From Equations (3), (4), (8) and (9):

$$\beta \geq \arctan \frac{1 - \mu_1 \mu_2}{\mu_1 + \mu_2} \tag{10}$$

The geometrical analysis from Figure 6 is as follows:

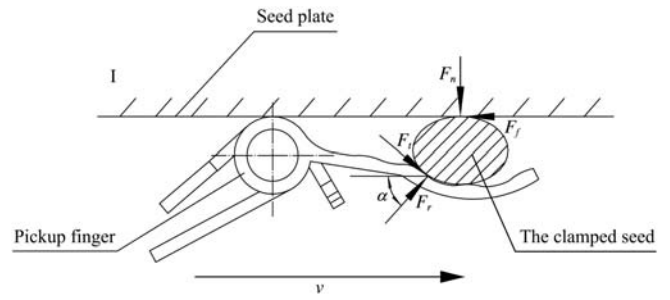
$$\theta = \pi - \alpha - \beta \tag{11}$$

From Equations (7), (10) and (11):

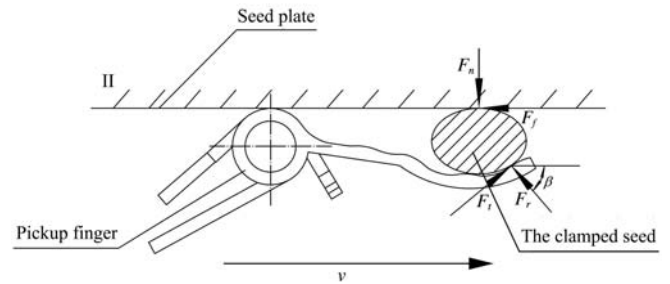
$$\theta \leq \pi - \left( \arctan \frac{1 + \mu_1 \mu_2}{\mu_2 - \mu_1} + \arctan \frac{1 - \mu_1 \mu_2}{\mu_1 + \mu_2} \right) \tag{12}$$

Above related parameters were substituted into the Equation (12), the wrap angle of finger arc-segment  $\theta$  should be less than  $53^\circ$ .

To analyze the clamping performance of ripple surface type pickup finger, a research was conducted on the seed that relative slippages occurred in the clamping and pushing processes. The model was simplified from the process of actual clamping movement, as shown in Figure 7.



a. Seed clamped in the limit position I



b. Seed clamped in the limit position II

Note:  $F_n$  is the support of seed forced by seed plate, N;  $F_f$  is the friction of seed forced by seed plate, N;  $F_r$  is the friction of seed forced by pickup finger, along the tangential direction of the internal ripple surface, N;  $F_t$  is the support of seed forced by pickup finger, along the axial direction of the internal ripple surface, N;  $\alpha$  and  $\beta$  are the angles between the horizontal direction and the support force by pickup finger in the limit position I, II respectively, ( $^\circ$ ).

Figure 6 Diagram of forces system on the clamped seed

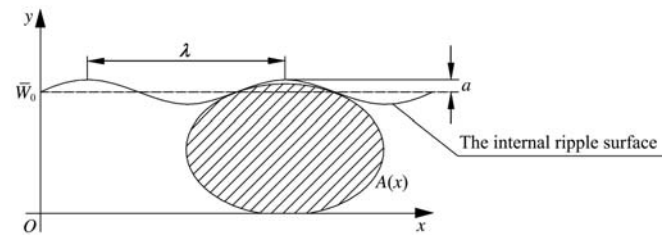


Figure 7 Analysis of the clamping performance

The equation of generatrix of internal ripple surface is given by:

$$y = \bar{W}_0 + a \sin \frac{2\pi x}{\lambda} \tag{13}$$

Cross-sectional area  $A(x)$  of the clamped seed is:

$$A(x) = \frac{\pi}{4} (\bar{W}_0 + a \sin \frac{2\pi x}{\lambda})^2 \tag{14}$$

where,  $\bar{W}_0$  is the average value of generatrix;  $A(x)$  is the cross-sectional area of the clamped seed,  $\text{mm}^2$ , its approximate value is  $\pi \bar{W}_0$ .

In the clamping and pushing processes, the forces on the clamped seed in the vertical direction ( $y$ -axis) are supposed to reach balance. The relative displacement which occurred between pickup finger and seed is caused by the resultant force in the horizontal direction ( $x$ -axis). The slippage  $\Delta L$  in the horizontal direction of the

clamped seed is given by:

$$\Delta L = \int_0^l \frac{P_H}{EA(x)} dx \quad (15)$$

where,  $P_H$  is the resultant force on the clamped seed by the ripple surface type pickup finger in the horizontal direction, N;  $E$  is elastic Modulus, MPa.

Combining Equations (14) and (15) derived the following formula:

$$\Delta L = \frac{4P_H}{E\pi} \int_0^l \frac{1}{(\bar{W}_0 + a \sin \frac{2\pi x}{\lambda})^2} dx \quad (16)$$

To contrast and analyze the clamping performance of ripple surface type pickup finger, the original smooth surface type pickup finger was selected as a reference.

When the seed is clamped by the original pickup finger, it will produce the slippage  $\Delta L'$  in the horizontal direction,  $\Delta L'$  can be expressed as:

$$\Delta L' = \int_0^l \frac{P'_H}{EA(x)} dx = \frac{4P'_H}{E\pi} \int_0^l \frac{1}{\bar{W}_0^2} dx \quad (17)$$

where,  $P'_H$  is the resultant force on the clamped seed by the original pickup finger in the horizontal direction, N.

Supposing the slippage  $\Delta L$  is equal to the slippage  $\Delta L'$ :

$$\Delta L = \Delta L' \quad (18)$$

From Equations (16), (17) and (18):

$$K = \frac{P_H}{P'_H} = \frac{(\bar{W}_0 + a \sin \frac{2\pi x}{\lambda})^2}{\bar{W}_0^2} \times 100\% \quad (19)$$

where,  $K$  expresses that the energy of the ripple surface type pickup finger increased  $K$  times by the original pickup finger required, when the same slippage of clamped seed occurs. The performance of ripple surface type pickup finger improves  $K$  times.

Taking the ripple surface type pickup finger as an example, its structural parameters (the wavelength and amplitude of ripple surface  $\lambda$  and  $a$ ) were substituted into the Equation (19) to calculate  $K=11\%-24\%$ .

#### 4 EDEM numerical simulation experiment

In order to optimize the structural parameters of ripple surface type pickup finger and to test the seeding performance of seed metering device, the working process should be simulated well by the discrete element

software EDEM based on the discrete element method (DEM). Then numerical simulations of orthogonal experiments on seeding performance were conducted to verify the effects of these influencing factors on the quality of seeding.

##### 4.1 Establishment of geometric model

The parts which had no contact with seeds in the working process were removed to conveniently simulate and calculate. The geometric model was created by Pro/E software and imported into EDEM software in .igs format, as shown in Figure 8. The elastic function was compiled by C-language, and the elastic force was loaded by the API (Application Programming Interface) of EDEM software<sup>[11]</sup>. The simulation materials and physical parameters of seed metering device were set as shown in Table 1. These data were obtained based on physics experimental determination and some references<sup>[12-14]</sup>.



Figure 8 Geometric model of pickup finger precision maize seed metering device

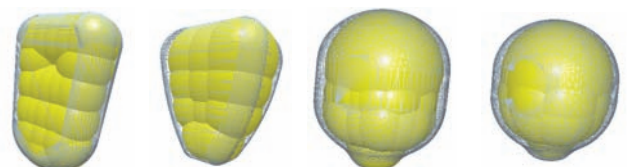
Table 1 Simulation parameters of metering device

| Items          | Materials       | Physical parameters |                      |                            |
|----------------|-----------------|---------------------|----------------------|----------------------------|
|                |                 | Poisson's ratio     | Shear modulus /Pa    | Density /kg·m <sup>3</sup> |
| Pickup finger  | Aluminium alloy | 0.42                | $1.7 \times 10^{10}$ | 2700                       |
| Seed plate     | 65Mn            | 0.30                | $7.8 \times 10^{10}$ | 7850                       |
| Cleaning brush | Bristle         | 0.40                | $1.0 \times 10^8$    | 1150                       |

##### 4.2 Establishment of maize seed model

In order to more actually simulate maize seeds, the three-dimensional models of four grades of maize seeds were established in Pro/E software based on the dimension size distributions. The virtual particles were filled by the spherical combination method<sup>[15]</sup> in EDEM software, as shown in Figure 9. This combined sphere could simulate maize seeds satisfactorily. Supposing the physical parameters of each type of maize seeds remained

consistent to simply calculation. The characteristics of maize seeds such as Poisson’s ratio, shear modulus, density, coefficient of restitution, coefficient of static friction and coefficient of dynamic friction among seeds were set to 0.357,  $2.17 \times 10^8$  Pa,  $1250 \text{ kg/m}^3$ , 0.6, 0.5 and  $0.01^{[16]}$ .



a. Big flat seed b. Small flat seed c. Big round seed d. Small round seed  
Figure 9 EDEM particle models of maize seeds

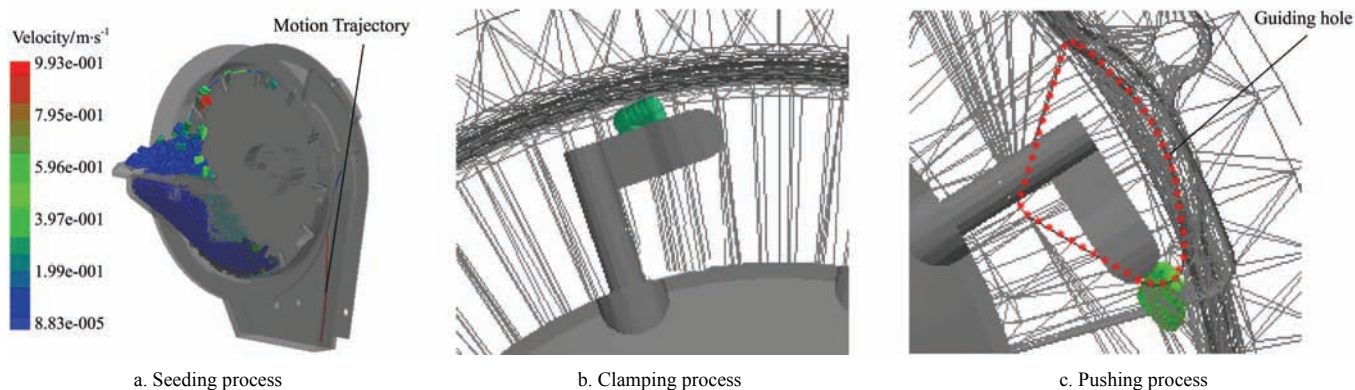
**4.3 Setting of simulation and calculation**

Due to maize seeds had no adhesive action, Hertz-Mindlin no-slip model<sup>[17]</sup> was used to show the mechanics relation between seeds and parts. The amount of maize seeds was set to generate 1000 particles per second according to seed-filling requirements. The initial velocity of particles was 0 m/s, the total number of particles was 1500, the time of generating particles was 1.5 s, and the total time of whole simulation was 20 s. The data storage time was to perform iteration storage once every 0.5 s. The grid size was set as doubling the

minimum size in the dropping hole to calculate experimental indexes of seeding performance.

**4.4 Seeding process of numerical simulation**

The single particle model of maize seed was taken as the study object and displayed in the streamline form. We got a picture cut from the simulation process as shown in Figure 10a. The colorful streamline indicated the motion trajectory of the tracked particle, and different colors of streamline indicated the changes of its velocity. Through analyzing the streamline states, the clear motion rules of maize seeds could be obtained. With the rotation of seed finger plate, the movements of maize seeds in the edge of filling zone were more obvious, and the velocity of boundary layer was increased gradually. The above phenomenon was consistent with the actual working condition. We set the guiding room that located in the back of seed metering device to display in mesh form for conveniently observing the simulation processes of clamping, pushing and guiding. The condition of single seed clamped in the simulation process, is shown in Figure 10b, and the condition of single seed pushed to the guiding hole is shown in Figure 10c.



a. Seeding process b. Clamping process c. Pushing process  
Figure 10 EDEM simulation processes of seed metering

**4.5 Factors and response indexes**

In order to examine the working performance of seed metering device and obtain better structural parameters of ripple surface type pickup finger, we selected four types of maize seeds as the research objects to conduct four groups of numerical orthogonal seeding experiments respectively. According to the theoretical analysis, the number of factors and the consideration of interactions among factors, the rotational speed of seed metering

device  $n$ , wavelength of ripple surface  $\lambda$  and amplitude of ripple surface  $a$  were selected as the experimental factors. The numerical simulations of orthogonal seeding experiments were carried out through changing the parametric models. Combined with above theoretical analysis, requirements of actual operating rotation speed and single factor experiments, we determined the variation ranges of three factors. The factors and levels are as shown in Table 2.

**Table 2 Factors and levels of simulation experiments**

| Levels | Factors  |  |   |
|--------|--|--|---|
|        | Rotational speed<br><i>A</i> /(r·min <sup>-1</sup> ) | Wavelength of ripple<br>surface <i>B</i> /mm | Amplitude of ripple<br>surface <i>C</i> /mm |
| 1      | 20   | 6  | 2.0   |
| 2      | 25   | 8  | 2.6   |
| 3      | 30   | 10   | 3.2   |

According to GB/T 6973-2005 “Test method of single seed drills (precision drills)”<sup>[18]</sup> and JB/T 10293-2001 “Specifications of single seed drills (precision drills)”<sup>[19]</sup> in China, the evaluation indexes were the average qualified index and the seeding coefficient of variation in four different types of maize seeds. The calculation equations are as follows:

$$S_i = \frac{n_i}{N} \times 100\% \quad (i=1,2,3,4) \quad (20)$$

$$C_i = \sigma_i \times 100\% \quad (i=1,2,3,4) \quad (21)$$

$$\bar{S} = \frac{1}{4} \sum_{i=1}^{i=4} S_i \quad (22)$$

$$\bar{C} = \frac{1}{4} \sum_{i=1}^{i=4} C_i \quad (23)$$

where, *N* is the theoretical number of seeding; *n*<sub>1</sub> is the number of single seeding;  $\sigma$  is the standard deviation; *S*<sub>1</sub> is the seeding qualified index of big flat seed; *S*<sub>2</sub> is the seeding qualified index of small flat seed; *S*<sub>3</sub> is the seeding qualified index of big round seed; *S*<sub>4</sub> is the seeding qualified index of small round seed; *C*<sub>1</sub> is the seeding coefficient of variation of big flat seed; *C*<sub>2</sub> is the seeding coefficient of variation of small flat seed; *C*<sub>3</sub> is the seeding coefficient of variation of big round seed; *C*<sub>4</sub> is the seeding coefficient of variation of small round seed.

**4.6 Results and discussion**

By evaluating the interactions among different factors, the orthogonal array L<sub>27</sub>(3<sup>13</sup>) was used to arrange the experiments<sup>[20-22]</sup>. The schemes and results of experiments were analyzed by using Design-Expert 6.0 software, as shown in Table 3. Thus the data could be analyzed by analysis of variance (ANOVA), as shown in Table 4.

**Table 3 Schemes and results of simulation experiments**

| No.       | Factors               |          |                                      |                                      |          |                                      |                                      |                                      |                                      | Test evaluation indexes/% |   |
|-----------|-----------------------|----------|--------------------------------------|--------------------------------------|----------|--------------------------------------|--------------------------------------|--------------------------------------|--------------------------------------|---------------------------|---|
|           | <i>A</i>              | <i>B</i> | ( <i>A</i> × <i>B</i> ) <sub>1</sub> | ( <i>A</i> × <i>B</i> ) <sub>2</sub> | <i>C</i> | ( <i>A</i> × <i>C</i> ) <sub>1</sub> | ( <i>A</i> × <i>C</i> ) <sub>2</sub> | ( <i>B</i> × <i>C</i> ) <sub>1</sub> | ( <i>B</i> × <i>C</i> ) <sub>2</sub> | $\bar{S}$                 | $\bar{C}$   |
| 1         | 1(20)                 | 1(6)     | 1                                    | 1                                    | 1(2.0)   | 1                                    | 1                                    | 1                                    | 1                                    | 93.31                     | 12.64   |
| 2         | 1                     | 1        | 1                                    | 1                                    | 2(2.6)   | 2                                    | 2                                    | 2                                    | 2                                    | 90.64                     | 14.88   |
| 3         | 1                     | 1        | 1                                    | 1                                    | 3(3.2)   | 3                                    | 3                                    | 3                                    | 3                                    | 88.27                     | 16.91   |
| 4         | 1                     | 2(8)     | 2                                    | 2                                    | 1        | 1                                    | 1                                    | 2                                    | 3                                    | 93.05                     | 12.31   |
| 5         | 1                     | 2        | 2                                    | 2                                    | 2        | 2                                    | 2                                    | 3                                    | 1                                    | 92.16                     | 13.98   |
| 6         | 1                     | 2        | 2                                    | 2                                    | 3        | 3                                    | 3                                    | 1                                    | 2                                    | 92.01                     | 12.76   |
| 7         | 1                     | 3(10)    | 3                                    | 3                                    | 1        | 1                                    | 1                                    | 3                                    | 2                                    | 92.91                     | 11.09   |
| 8         | 1                     | 3        | 3                                    | 3                                    | 2        | 2                                    | 2                                    | 1                                    | 3                                    | 92.36                     | 15.98   |
| 9         | 1                     | 3        | 3                                    | 3                                    | 3        | 3                                    | 3                                    | 2                                    | 1                                    | 88.58                     | 11.90   |
| 10        | 2(25)                 | 1        | 2                                    | 3                                    | 1        | 2                                    | 3                                    | 1                                    | 1                                    | 94.45                     | 12.30   |
| 11        | 2                     | 1        | 2                                    | 3                                    | 2        | 3                                    | 1                                    | 2                                    | 2                                    | 92.38                     | 12.86   |
| 12        | 2                     | 1        | 2                                    | 3                                    | 3        | 1                                    | 2                                    | 3                                    | 3                                    | 93.31                     | 13.36   |
| 13        | 2                     | 2        | 3                                    | 1                                    | 1        | 2                                    | 3                                    | 2                                    | 3                                    | 93.35                     | 11.23   |
| 14        | 2                     | 2        | 3                                    | 1                                    | 2        | 3                                    | 1                                    | 3                                    | 1                                    | 93.89                     | 10.73   |
| 15        | 2                     | 2        | 3                                    | 1                                    | 3        | 1                                    | 2                                    | 1                                    | 2                                    | 92.25                     | 10.56   |
| 16        | 2                     | 3        | 1                                    | 2                                    | 1        | 2                                    | 3                                    | 3                                    | 2                                    | 89.78                     | 11.53   |
| 17        | 2                     | 3        | 1                                    | 2                                    | 2        | 3                                    | 1                                    | 1                                    | 3                                    | 90.04                     | 13.48   |
| 18        | 2                     | 3        | 1                                    | 2                                    | 3        | 1                                    | 2                                    | 2                                    | 1                                    | 89.17                     | 14.18   |
| 19        | 3(30)                 | 1        | 3                                    | 2                                    | 1        | 3                                    | 2                                    | 1                                    | 1                                    | 90.34                     | 16.11   |
| 20        | 3                     | 1        | 3                                    | 2                                    | 2        | 1                                    | 3                                    | 2                                    | 2                                    | 89.78                     | 16.03   |
| 21        | 3                     | 1        | 3                                    | 2                                    | 3        | 2                                    | 1                                    | 3                                    | 3                                    | 86.01                     | 13.72   |
| 22        | 3                     | 2        | 1                                    | 3                                    | 1        | 3                                    | 2                                    | 2                                    | 3                                    | 92.26                     | 13.01   |
| 23        | 3                     | 2        | 1                                    | 3                                    | 2        | 1                                    | 3                                    | 3                                    | 1                                    | 92.45                     | 13.23   |
| 24        | 3                     | 2        | 1                                    | 3                                    | 3        | 2                                    | 1                                    | 1                                    | 2                                    | 91.58                     | 12.01   |
| 25        | 3                     | 3        | 2                                    | 1                                    | 1        | 3                                    | 2                                    | 3                                    | 2                                    | 91.34                     | 13.56   |
| 26        | 3                     | 3        | 2                                    | 1                                    | 2        | 1                                    | 3                                    | 1                                    | 3                                    | 85.23                     | 18.35   |
| 27        | 3                     | 3        | 2                                    | 1                                    | 3        | 2                                    | 1                                    | 2                                    | 1                                    | 87.56                     | 15.11   |
| $\bar{S}$ | <i>K</i> <sub>1</sub> | 91.48    | 90.94                                | 90.83                                | 90.65    | 92.31                                | 91.27                                | 91.19                                | 91.29                                | 91.32                     | <i>A</i> <sub>2</sub> <i>B</i> <sub>2</sub> <i>C</i> <sub>1</sub> |
|           | <i>K</i> <sub>2</sub> | 92.07    | 92.56                                | 91.28                                | 90.26    | 90.99                                | 90.87                                | 91.54                                | 90.75                                | 91.41                     |   |
|           | <i>K</i> <sub>3</sub> | 89.61    | 89.67                                | 91.05                                | 92.25    | 89.86                                | 91.01                                | 90.43                                | 91.12                                | 90.43                     |   |
|           | <i>R</i>              | 2.46     | 2.89                                 | 0.45                                 | 1.99     | 2.45                                 | 0.396                                | 1.11                                 | 0.54                                 | 0.89                      |   |
| $\bar{C}$ | <i>K</i> <sub>1</sub> | 13.61    | 14.20                                | 13.54                                | 13.77    | 12.52                                | 13.54                                | 12.66                                | 13.67                                | 13.28                     | <i>A</i> <sub>2</sub> <i>B</i> <sub>2</sub> <i>C</i> <sub>1</sub> |
|           | <i>K</i> <sub>2</sub> | 12.25    | 12.20                                | 13.84                                | 13.67    | 14.40                                | 13.42                                | 13.83                                | 13.51                                | 12.81                     |   |
|           | <i>K</i> <sub>3</sub> | 14.45    | 13.91                                | 12.92                                | 12.86    | 13.39                                | 13.35                                | 13.81                                | 13.12                                | 14.26                     |   |
|           | <i>R</i>              | 2.20     | 2.00                                 | 0.92                                 | 0.91     | 1.88                                 | 0.19                                 | 1.17                                 | 0.55                                 | 1.45                      |   |

Note: *A*, *B*, *C* mean coded values of the rotational speed, the wavelength and amplitude of ripple surface respectively.  $\bar{S}$ ,  $\bar{C}$  mean values of the average seeding qualified index and the average seeding coefficient of variation of maize seeds in 4 different types respectively. *K*<sub>1</sub>, *K*<sub>2</sub>, *K*<sub>3</sub> mean the average values of each level respectively.

**Table 4 Results of ANOVA**

| Test index                               | Variation source | Standard deviation square | Degree of freedom | Mean square <i>MS</i> | F value | Significance |
|--|------------------|---------------------------|-------------------|-----------------------|---------|--------------|
| Average seeding qualified index          | <i>A</i>         | 29.47                     | 2                 | 14.74                 | 6.28    | *            |
|  | <i>B</i>         | 37.81                     | 2                 | 18.90                 | 8.05    | **           |
|  | <i>C</i>         | 27.06                     | 2                 | 14.53                 | 5.76    | *            |
| Average seeding coefficient of variation | <i>A</i>         | 24.05                     | 2                 | 12.25                 | 9.15    | ***          |
|  | <i>B</i>         | 22.58                     | 2                 | 11.29                 | 8.44    | **           |
|  | <i>C</i>         | 13.86                     | 2                 | 6.93                  | 5.18    | **           |

Note: \*\*\* means highly significance; \*\* means significance; \* means relative significance.

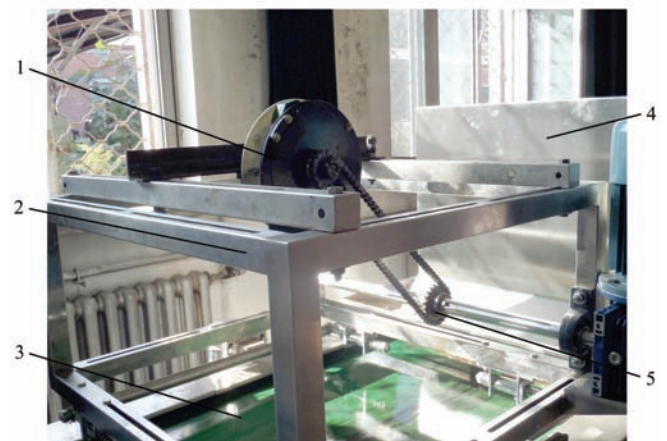
For all types of maize seeds, the greater average seeding qualified index means the better adaptability and comprehensive seeding performance, and the smaller average seeding coefficient of variation indicates the better stable seeding performance. From Table 3, the rules can be obtained in which the primary and secondary effect orders of each factor on the objective functions. The effect intensity of factors on the average seeding qualified index was that the wavelength of ripple surface *B* > the rotational speed *A* > the amplitude of ripple surface *C*. The effect intensity of factors the average seeding coefficient of variation was that the rotational speed *A* > the wavelength of ripple surface *B* > the amplitude of ripple surface *C*. According to the results of ANOVA, for the whole seeding performance, the rotational speed *A* and the wavelength of ripple surface *B* were significant impact factors, the amplitude of ripple surface *C* was relative significant impact factor.

The rule should be followed that the higher average seeding qualified index and lower average seeding coefficient of variation can obtain better structural parameters of ripple surface type pickup finger. The optimum combination of parameters was determined as  $A_2B_2C_1$ , from which the average seeding qualified index was 93.35% and the average seeding coefficient of variation was 11.23% under conditions of the 25 r/min rotational speed, 8 mm wavelength of ripple surface and 2 mm amplitude of ripple surface.

**5 Verification experiment**

In order to verify the truth and reliability of theoretical analysis and numerical simulations, the bench test was conducted in seeding performance laboratory of Northeast Agricultural University. Four different types of maize seeds were selected as the material of

conventional test. The test prototype was the improved pickup finger precision maize seed metering device installed with ripple surface type pickup finger. Based on the above optimization results, the structural parameters of ripple surface type pickup finger were as follows: the length of seed-finger clip was  $l=20.0$  mm, the width of finger clip was  $b=11.5$  mm, the length of finger arc-segment was  $l_1=13.0$  mm, the wavelength of ripple surface was  $\lambda=8.0$  mm and the amplitude of ripple surface was  $a=2.0$  mm. The test equipment is JPS-12 type of seed metering performance testing bench (Heilongjiang Agricultural Machinery Engineering Science Department)<sup>[23]</sup>, as shown in Figure 11.



1. Pickup finger precision maize seed metering device 2. Test bench 3. Seed bed 4. Image acquisition processing equipment 5. Transmission system

Figure 11 Actual operation of verification experiment

In the tests, the rotational speeds of seed metering device were set at 15 r/min, 20 r/min, 25 r/min, 30 r/min, 35 r/min, 40 r/min and 45 r/min, respectively. The seeding qualified index and seeding coefficient of variation of maize seeds were selected as experiment response indexes. The tests for each type of maize seeds were repeated three times, the average of data was processed as the final results, as shown in Table 5.

From Table 5, it can be found that, with the increase

of rotational speed, the seeding performance declined for all types of maize seeds, and the best seeding quality of small flat seed was obtained at the rotational speed of 15-45 r/min, which was greater than 87%. The seeding quality of small round seed was the worst; its qualified

index was greater than 83%. As the rotational speed was greater than 45 r/min, the seeding coefficient of variation of small round seed was over 20%, which indicated the clamping performance under this condition was instability.

**Table 5 Results of verification experiments**

| Rotational speed<br>(r·min <sup>-1</sup> ) | Big flat seed      |                            | Small flat seed    |                            | Big round seed     |                            | Small round seed   |                            |
|--|--------------------|----------------------------|--------------------|----------------------------|--------------------|----------------------------|--------------------|----------------------------|
|  | Qualified index /% | Coefficient of variation/% |
| 15   | 93.75              | 11.03                      | 95.12              | 9.87                       | 92.84              | 12.76                      | 91.83              | 13.26                      |
| 20   | 92.15              | 11.87                      | 94.65              | 10.64                      | 92.01              | 13.11                      | 90.15              | 14.45                      |
| 25   | 91.68              | 12.35                      | 93.37              | 11.68                      | 91.43              | 13.59                      | 89.76              | 15.13                      |
| 30   | 90.53              | 13.50                      | 92.51              | 12.16                      | 90.34              | 14.78                      | 87.97              | 16.03                      |
| 35   | 88.99              | 14.37                      | 91.29              | 12.95                      | 88.36              | 15.17                      | 86.40              | 16.57                      |
| 40   | 86.50              | 15.11                      | 88.01              | 13.51                      | 86.14              | 15.54                      | 85.27              | 17.89                      |
| 45   | 85.11              | 15.87                      | 87.23              | 14.27                      | 84.75              | 16.59                      | 83.04              | 19.92                      |

As the rotational speed was 25 r/min, the average seeding qualified index of was 91.56%, the average seeding coefficient of variation was 13.19%, and the maximum error of the qualified index between test and simulation results was 1.95%. The main reason of error may be that the shape and size of each type of maize seeds are completely same in numerical simulations, but there are still differences in actual test even after manual classification of cleaning. And there is a vibration of machine running in the process of operation. But the total errors can be acceptable. The qualified index of the improved seed metering device exceeded the original one by 12.34%, which could meet the requirements of precision seeding.

## 6 Conclusions

1) Taking pickup finger precision maize seed metering device as the research object, the main structure and working principle of seed metering device were detailed. The dimension size distributions of maize seeds in different types were studied, the gestures of seeds clamped by pickup finger were analyzed, and the clamping dynamical model of pickup finger was established by theoretical analysis. And then a ripple surface type pickup finger was designed to improve the seeding performance of pickup finger precision maize seed metering device and provide a solution for problems on precision maize planter.

2) The numerical simulations of orthogonal seeding performance experiments were conducted to verify the effects of these influencing factors on the quality of seeding. The results showed that the effect of intensity of factors on the seeding performance was the wavelength of ripple surface  $B >$  the rotational speed  $A >$  the amplitude of ripple surface  $C$ . The average seeding qualified index was 93.35% and the average seeding coefficient of variation was 11.23% under conditions of the 25 r/min rotational speed, 8 mm wavelength of ripple surface and 2 mm amplitude of ripple surface.

3) The bench test was conducted to verify the truth and reliability of theoretical analysis and numerical simulations. The results showed that with the increase of rotational speed, the seeding quantity declined for all types of maize seeds. The qualified index of the improved seed metering device exceeded the original one by 12.34%. The working performance can meet the requirements of precision maize seeding.

## Acknowledgements

The authors acknowledge that this research was financially supported by the National Science and Technology Support Plan Project (2014BAD06B04).

## [References]

- [1] Yang L, Yang B X, Cui T, Yu Y M, He X T, Liu Q W, et al. Global overview of research progress and development of

- precision maize planters. *Int J Agric & Biol Eng*, 2016; 9(1): 9–16.
- [2] Searle C L, Kocher M F, Smith J A, Blankenship E E. Field slope effects on uniformity of corn seed spacing for three precision planter metering systems. *Transactions of the ASABE*, 2008; 24(5): 581–586.
- [3] Finger pickup plateless seed meter. Available: [http://salesmanual.deere.com/sales/salesmanual/en\\_NA/seeding/2009/feature/metering/deeraplant/m\\_e\\_finger\\_pickup\\_meter.html](http://salesmanual.deere.com/sales/salesmanual/en_NA/seeding/2009/feature/metering/deeraplant/m_e_finger_pickup_meter.html). Accessed on [2016-01-16].
- [4] Wang J W, Tang H, Zhou W Q, Yang W P, Wang Q. Improved design and experiment on pickup finger precision seed metering device. *Transactions of the CSAM*, 2015; 46(9): 68–76. (in Chinese)
- [5] Wang J W, Tang H, Wang Q, Zhou W Q, Yang W P, Shen H G. Numerical simulation and experiment on seeding performance of pickup finger precision seed metering device based on EDEM. *Transactions of the CSAE*, 2015; 31(21): 43–50. (in Chinese)
- [6] Liu J, Cui T, Zhang D X, Yang L, Gao N N, Wang B. Effects of maize seed grading on sowing quality by pneumatic precision seeding-metering device. *Transactions of the CSAE*, 2010; 26(9): 109–113. (in Chinese)
- [7] Liu H X, Guo L F, Fu L L, Tang S F. Study on multi-size seed metering device for vertical plate soybean precision planter. *Int J Agric & Biol Eng*, 2015; 8(1): 1–8.
- [8] Shi S, Zhang D X, Yang L, Cui T, Li K H. Simulation and verification of seed-filling performance of pneumatic combined holes maize precision seed metering device based on EDEM. *Transactions of the CSAE*, 2015; 31(3): 62–69. (in Chinese)
- [9] Liu H X, Xu X M, Guo L F, Sang J J. Research on seed-filling mechanism of vertical shallow basin type seed metering device with composite filling force. *Transactions of the CSAE*, 2014; 30(21): 9–16. (in Chinese)
- [10] Dun G Q, Chen H T, Feng Y N, Yang J L, Li A, Zha S H. Parameter optimization and test of key parts of fertilizer allocation device based on EDEM software. *Transactions of the CSAE*, 2016; 32(7): 36–42. (in Chinese)
- [11] Yang L, He X T, Cui T, Zhang D X, Shi S, Zhang R, et al. Development of mechatronic driving system for seed meters equipped on conventional precision corn planter. *Int J Agric & Biol Eng*, 2015; 8(4): 1–9.
- [12] Shi L R, Wu J M, Sun W, Zhang F W, Sun B G, Liu Q W. Simulation test for metering process of horizontal disc precision metering device based on discrete element method. *Transactions of the CSAE*, 2014; 30(8): 40–48. (in Chinese)
- [13] Yu J J, Liao Y Y, Cong J L, Yang S, Liao Q X. Simulation analysis and match experiment on negative and positive pressures of pneumatic precision metering device for rapeseed. *Int J Agric & Biol Eng*, 2014; 7(3): 1–12.
- [14] Qi B, Zhang D X, Cui T. Design and experiment of central pneumatic seed meter for maize. *Transactions of the CSAE*, 2013; 29(18): 8–15. (in Chinese)
- [15] Liao Q X, Zhang P L, Liao Y T, Yu J J, Cao X Y. Numerical simulation on seeding performance of centrifugal rape-seed metering device based on EDEM. *Transactions of the CSAM*, 2014; 45(2): 109–114. (in Chinese)
- [16] Huang X M, Zha X T, Pan H B, Zhong W Y, Chen H. Measurement and analysis of rapeseed's restitution coefficient in point-to-plate collision model. *Transactions of the CSAE*, 2014; 30(24): 22–29. (in Chinese)
- [17] Yang S D, Zhang D X, Gao Z Q, Liu X J. Flow field simulation and working parameters analysis of side positive pressure maize seeding device. *Transactions of the CSAM*, 2015; 46(9): 41–45. (in Chinese)
- [18] GB/T 6973-2005 Testing method of single seed drills (precision drills). National Standards of the People's Republic of China. (in Chinese)
- [19] JB/T 10293-2001 Specifications of single seed drills (precision drills). Machinery Industry Standards of the People's Republic of China. (in Chinese)
- [20] Lü J Q, Yang Y, Li Z H, Shang Q Q, Li J C, Liu Z Y. Design and experiment of an air-suction potato seed metering device. *Int J Agric & Biol Eng*, 2016; 9(5): 33–42.
- [21] Zhang G Z, Zang Y, Luo X W, Wang Z M, Zhang Q, Zhang S S. Design and indoor simulated experiment of pneumatic rice seed metering device. *Int J Agric & Biol Eng*, 2015; 8(4): 10–18.
- [22] Yang S, Zhang S M. Design and parameter optimization of flexible comb-type grass seed metering device. *Int J Agric & Biol Eng*, 2015; 8(1): 9–16.
- [23] Tian L Q, Wang J W, Tang H, Li S W, Zhou W Q, Shen H G. Design and performance experiment of helix grooved rice seeding device. *Transactions of the CSAM*, 2016; 47(5): 46–52. (in Chinese)